

## SSR mitigation with SSSC thanks to fuzzy control

Seyed Mohammad Hassan HOSSEINI, Hadi SAMADZADEH,\* Javad OLAMAEI,  
Murtaza FARSADI

Islamic Azad University, Tehran, Tehran, Iran

Received: 05.03.2012 • Accepted: 01.08.2012 • Published Online: 30.10.2013 • Printed: 25.11.2013

**Abstract:** This paper deals with the capability of a static synchronous series compensator (SSSC) to attenuate the subsynchronous resonance (SSR). Two well-known controllers are designed, namely a conventional damping controller (CDC) and fuzzy logic damping controller (FLDC). These 2 damping controllers are added to a main control loop of a SSSC operating as a SSR damping controller. It should be noted that, to optimize the parameters of the CDC, a versatile optimization technique is implemented, namely particle swarm optimization (PSO). A comprehensive comparison between the 2 control methods is carried out for different operational conditions. To observe the superior performance of the proposed FLDC, many operating points and different fault types are considered. The IEEE second benchmark model aggregated with the SSSC is utilized and simulations are presented.

**Key words:** Flexible AC transmission systems, fuzzy logic control, static synchronous series compensator, particle swarm optimization, subsynchronous resonance

### 1. Introduction

The method of series compensation for long transmission lines is one of the economical techniques to improve the power transmission capability and also to increase the maximum power tracking of these lines [1]. The frequently occurring subsynchronous resonance (SSR) phenomena [2–3] can be described with the interactions between electrical modes of the series compensated network and a mechanical shaft mode of a turbine generator. The first SSR was reported at the Mohave Station in the early 1970s [4]. Nowadays, the SSR has emerged as one of the challenging topics in the field of power system dynamics. A vase body structure is utilized to implement various devices such as power system stabilizers (PSSs) [5] and flexible alternating current transmission systems (FACTS) [6–12] to mitigate the SSR problem.

The static synchronous series compensator (SSSC) is one of the FACTS devices utilized by a gate turn-off thyristor-based voltage source inverter yielding controllable compensating voltage over an identical capacitive and inductive range that is independent of the magnitude of the line current [13,14].

Several efforts have been investigated on the torsional performance of SSSC and also for designing a supplementary damping controller used in damping the SSR. As an example, the performance of the SSSC stated in the IEEE First Benchmark Model was examined in [15] and it was shown that an incremental value of the conventional fixed series capacitor compensation could increase the damping of small signal oscillations though the damping level of the SSSC, which remains almost constant at a lower level. The effects of the DC link capacitor value used in the SSSC for the torsional modes were also studied. In [16], a robust controller

\*Correspondence: h\_samadzadeh@yahoo.com

based on the optimal  $H_\infty$  control theory was used to improve the torsional performance of SSSC. In [17,18], Bongiorno et al. discussed a novel control strategy for SSR attenuation by increasing the network damping only at those frequencies that are critical for the turbine-generator shaft. El-Moursi et al. [9] proposed a novel controller for reduction of SSR with the aid of SSSC.

Most efforts that have been focused on auxiliary damping controllers designed for SSSCs are based on a linearized system model. The controller parameters were tuned to some nominal operation states. In the matter of large disturbances, the system conditions exhibit extremely nonlinear behaviors in the sense that controllers have no chance to dampen the oscillations. In this condition, the controller may play the role of a destabilizing factor for the disturbances, for example by imposing negative damping [19]. The control design technique hence needs to utilize the nonlinear dynamics of the power system in order to overcome such undesirable problems. For this purpose, some stabilizing control methods of power systems were suggested [20]. The latest fuzzy control algorithm developed illustrates a systematic approach to control a nonlinear process based on human experience. This is considered as a heuristic approach improving the performance of the closed loop systems. A properly designed fuzzy controller yields a higher performance in the presence of variations for the parameters such as loads and external disturbances. It has been shown that fuzzy logic controllers (FLCs) play a drastic role in stabilizing power systems in a wide range of operating conditions and with various devices such as PSS and FACTS [21–23]. Consequently, the main contribution of this effort is to design a supplementary fuzzy logic damping controller (FLDC) for SSSC to mitigate the SSR. The FLDC is varied considerably with a suitable choice of membership functions and also parameters.

In order to determine the capabilities of the proposed controller, a comparison needs to be made between the designed controller and a conventional damping controller (CDC). Note that the parameters used in the CDC are optimized to yield better results. There are several methods to optimize the parameters of conventional classic controller, including the genetic algorithm (GA) [24] and particle swarm optimization (PSO) [25]. Recently, the PSO algorithm emerged as one of the powerful methods in managing optimization problems. PSO is counted as a population-based stochastic optimization algorithm, duplicated from the social behavior of birds or fish [26,27]. PSO not only eliminates the deficiencies of other conventional optimization methods, but it also utilizes few parameters and is easy to use. In this paper, the PSO algorithm is utilized to optimize the parameters of the CDC.

For both the FLDC and CDC, the design process is explained and a comprehensive comparison is conducted between 2 proposed controllers in various operation conditions, and then the results are thoroughly discussed.

## 2. System under study

The power system considered here is the IEEE SBM [28] aggregated with the SSSC as shown in Figure 1, which illustrates the single-line diagram of the power system used in this case study. A single generator of 600 MVA (22 kV) is connected to an infinite bus via a transformer and 2 parallel transmission lines. The mechanical subsystem is composed of 2-stage steam turbines (high pressure (HP) and low pressure (LP)), the generator (G), and the rotating exciter (EX). Note that all stated components are mounted on the same shaft, as shown in Figure 1. The compensation level provided by the series capacitor is set to 55% of the reactance  $X_{L1}$ . Different cases are here considered for clarifying the capabilities of the SSSC controllers:

- The case without the SSSC used in the system, where a 3-phase to the ground fault is applied at the generator bus (point A) at  $t = 0.1$  s and is then removed after 0.0168 s.

- The case including a SSSC linked to the compensated transmission line of the IEEE SBM and also 2 separate controllers designed for SSR reduction. Similar to the first case, a 3-phase to the ground fault occurs at  $t = 0.1$  s for 5 various durations and system operation points.

For the first case, the performance of the system without any kind of SSSC damping controllers is studied. The main contribution here is to validate the dominant mode of oscillations observed for the generator rotor shaft. It is also necessary to distinguish the rotor damages without any controller; the oscillations are hence expected to increase.

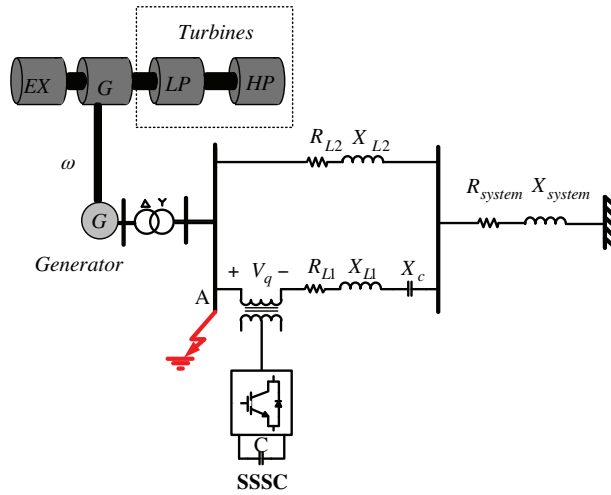


Figure 1. IEEE SBM model aggregated with SSSC.

### 2.1. Simulation results for the first case

Here we explain the transient simulation of the power system. The 3-phase to the ground fault occurs for 0.1 s and it then is removed after 0.0168 s, as shown in Figure 1. Figure 2 explains the simulation results for the rotor speed deviation ( $\Delta W$ ). Large oscillations exist between the sections of the turbine generator shaft due to the unstable modes observed for the fault cleared. Note that the system is completely unstable in this case.

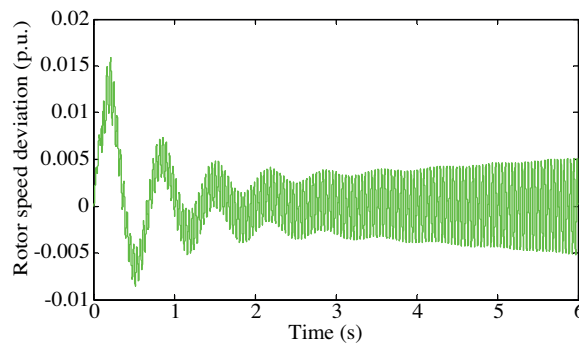


Figure 2. Simulation results for case 1, rotor speed deviation ( $\Delta W$ ) in p.u.

### 2.2. FFT analysis for the first case

The fast Fourier transform (FFT) is one of the powerful tools to determine the oscillatory modes of the system using MATLAB and for the IEEE SBM. Figure 3 shows the FFT plot of the generator rotor speed in the time

interval of 2 to 5 s. It is obvious that the complement of the electrical resonance frequency corresponds with the critical mode 1 of the IEEE SBM when the series compensation for line 1 is set to 55%, and the system hence shows unstable behaviors without any possible dampers. It can be distinguished that 3 modes exist in the rotor speed using the FFT analysis. Note that the second mode with the frequency of 25 Hz seems to be more unstable. On the other hand, the second torsional mode is the dominant mode for 55% compensation resulting from the subsynchronous frequency of 25 Hz.

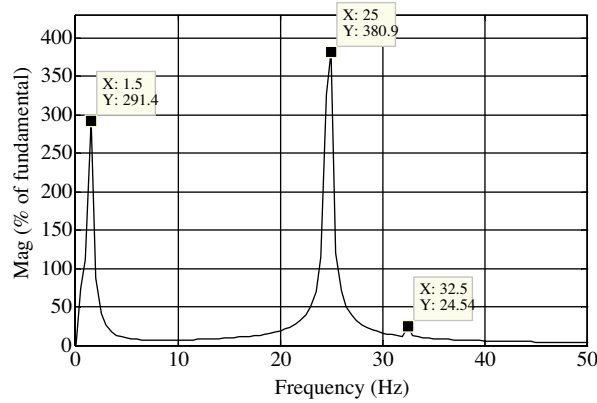


Figure 3. FFT analysis on the generator rotor shaft in order to validate the dominant mode.

The FFT analysis of the rotor speed is carried out for time interval of 2–6 s with a step time of 1 s to expand the subject of resonance and harsh impact of the dominant mode on the oscillations. The results obtained from FFT analysis are shown in Figure 4. This figure indicates significant incremental values of the dominant modes. Moreover, it is necessary to employ a controller to reduce this adverse oscillatory component from rotor shaft to keep the power system from suffering.

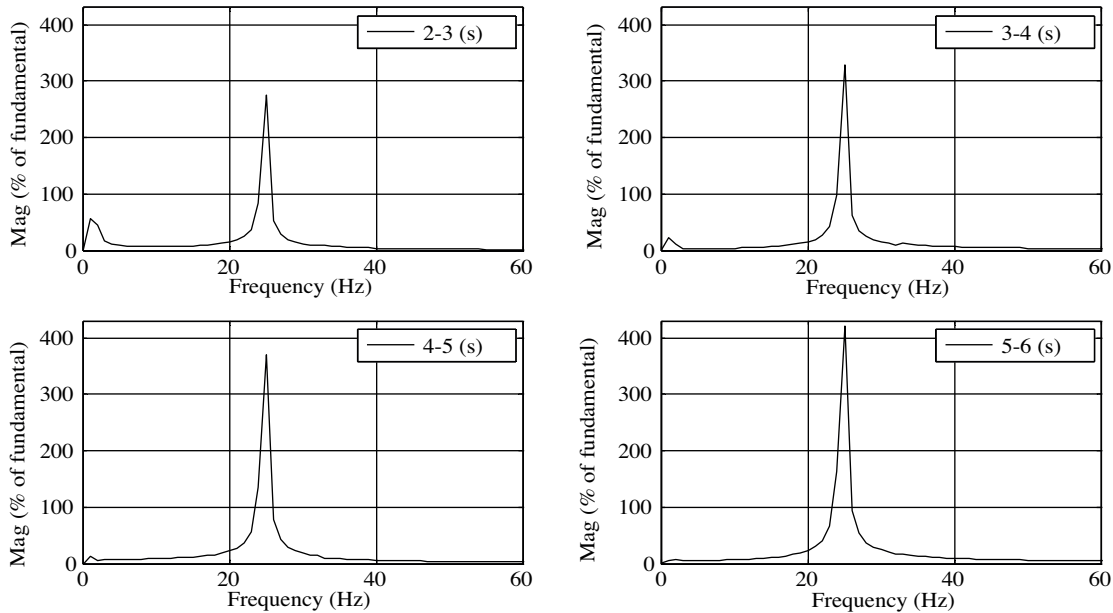
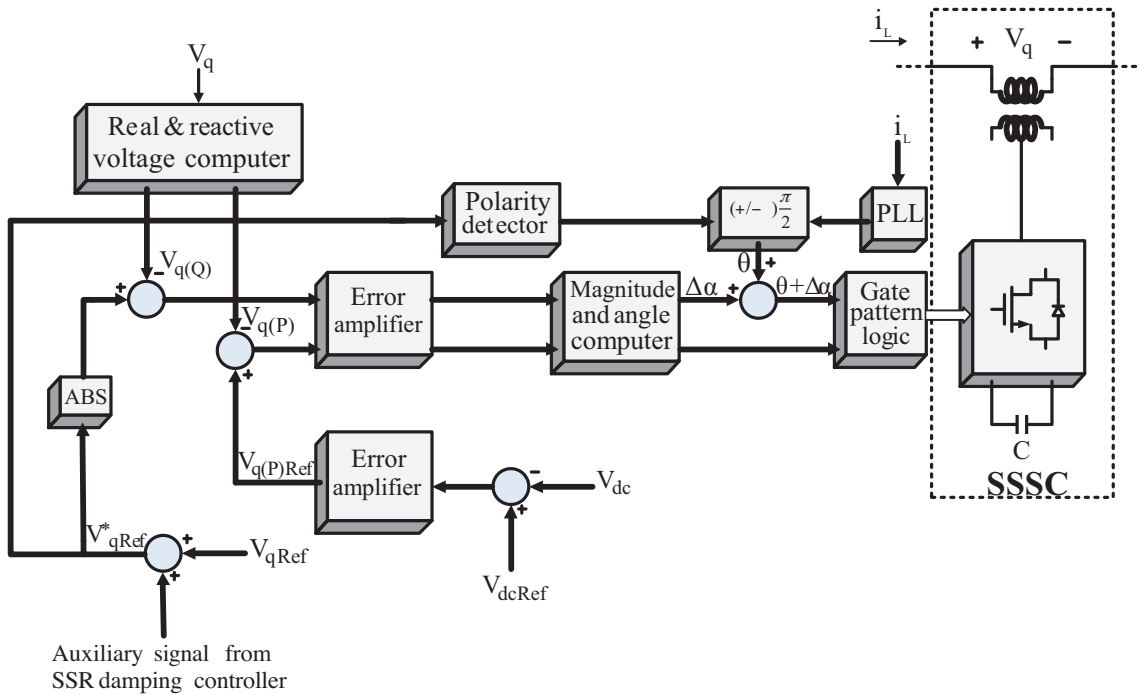


Figure 4. FFT analysis on  $\Delta\omega$  of the generator rotor speed without any controller.

**3. Controller design for the SSR mitigation**

This section deals with the SSSC control circuits to reduce the SSR. The SSSC is a well-known series-connected FACTS controller based on a voltage source converter (VSC). Figure 5 illustrates a typical SSSC model with a 3-phase VSC, a DC link capacitor, and an interfacing transformer. A filtering stage (not shown here) is also considered at the output of the VSC for alleviating the harmonic pollution in the injected voltage.



**Figure 5.** SSSC control system.

Indeed, the SSSC can be regarded as an advanced type of controlled series compensation. Figure 5 displays the main control system of the SSSC.  $V_{qref}$  is the desired magnitude of the series reactive voltage and determines the reactive power exchange for the series compensation. To be more precise, by injecting the series voltage, namely  $V_q$ , the SSSC provides a variable reactance  $X_q$  in series with the transmission line, which in turn is used to change the line reactance. In this way an active means of compensation, power flow control, as well as power oscillation damping, is achieved. The variable reactance realized by the SSSC is expressed as follows, where  $i_L$  denotes the line current [29].

$$X_q = \frac{V_q}{i_L} \tag{1}$$

The SSSC control system introduced above by itself does not provide the essential damping, since the primary task of the SSSC is to control the line power flow. However, the SSSC controllable signals can be modulated to achieve some other ancillary duties such as SSRD or power oscillation damping. In order to provide an effective damping of the SSR, it is necessary to apply coordinating tuning of the SSSC with the auxiliary SSRD controller.

Two cases designated as the CDC and FLDC are each scrutinized for showing controller abilities in the SSR mitigation of SSSC. The PSO algorithm is utilized to optimize the parameters of the CDC in order to improve the damping characteristics of the CDC and to compare the results with those of the FLDC. Time-

domain simulations are implemented to verify the superior performance of the FLDC toward its PSO-based CDC in SSR attenuation.

### 3.1. PSO-based CDC design

#### 3.1.1. PSO concept

The PSO method is a population-based stochastic optimization method that was developed by Kennedy and Eberhart in 1995. It was inspired by the social behavior of bird flocking or fish schooling [25]. This algorithm usually is utilized to ameliorate the speed of the convergence and also to detect the global optimum value of the objective function. It has the ability to solve many of the same problems similar to other optimization methods, such as the GA. In contrast with GAs, PSO is easy to implement, needs fewer adjustable parameters, is appropriate for the nature of the problem, and is easy for coding [25]. These plentiful merits that were cited have convinced researchers to select this kind of optimization method widely in power systems. PSO is launched with some initial random particles and searches for the optimal point with updating of generations.

In the search space of the PSO algorithm, particles, some of which are simple entities, are located. Each particle at its current position calculates the objective function and then determines its movement through the search space. The movement can be done by aggregating some facets of the history of the current and best position of the particles by other particles or more members of the swarm with some random perturbations. When all the particles have been moved, the next iteration will be happened. At last, the swarm, just like a school of fish that are collectively searching for food, is likely to move toward an optimum of the objective function [25,27].

As mentioned before, in the PSO technique a population of random solutions in a D-dimensional space is defined as particles. For instance, the  $i$ th particle is represented by  $X_i=(X_{i1},X_{i2},\dots,X_{id})$ . The coordinates of the particles that are associated with the fittest solution that is obtained so far are monitored in the hyperspace. The mentioned fitness value for the  $i$ th particle is stored as  $p_i=(p_{i1},p_{i2},\dots,p_{id})$ . Furthermore, the overall best value of the objective function obtained by the particles at the time ( $g$ best) is calculated through the algorithm. By dynamically regulating the velocity of each particle according to its own movement and the movement of the other particles, the trajectory of each individual in the search space is altered. The velocity vector of the  $i$ th particle in the D-dimensional search space can be expressed as  $V_i=(V_{i1},V_{i2},\dots,V_{id})$ . The optimization is achieved through changing the velocity of each particle toward its pbest and gbest at each step according to Eq. (1) [25]:

$$V_{id}(t) = w \times V_{id}(t-1) + c_1 r_1 \times (p_{id}(t-1) - X_{id}(t-1)) + c_2 r_2 \times (p_{gd}(t-1) - X_{id}(t-1)) \quad (2)$$

$$X_{id}(t) = X_{id}(t-1) + cV_{id}(t) \quad (3)$$

where,  $p_{id}$  and  $p_{gd}$  are pbest and gbest, respectively.  $c_1$  and  $c_2$  are positive constants that are responsible for variation of the particle velocity toward pbest and gbest.  $r_1$  and  $r_2$  are 2 random constants between 0 and 1. In order to balance the local and global searches and also to decrease the number of iterations,  $w$ , or the inertia weight, is defined. The definition of inertia weight is expressed as [25]:

$$w = w_{\max} - \frac{w_{\max} - w_{\min}}{\text{iter\_max}} \text{iteration}, \quad (4)$$

where iter\_max is the maximum number of iterations and iteration is the current number of iterations. The new inertia weight is updated through Eq. (4), where  $w_{\max}$  and  $w_{\min}$  are initial and final weights. The flowchart of the proposed PSO algorithm for the SSR study is shown in Figure 6.

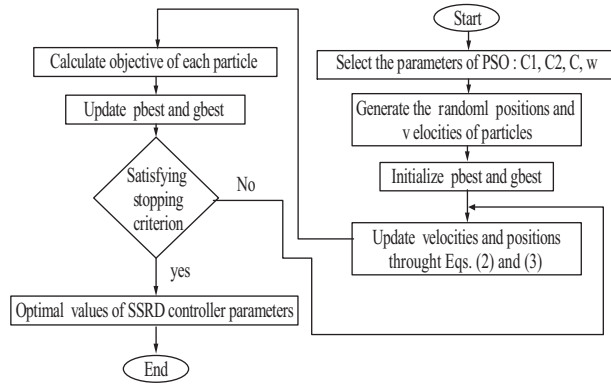


Figure 6. Flowchart of the proposed PSO algorithm for SSR attenuation.

3.1.2. Design of the PSO-based CDC

In order to improve the ability of the SSSC in SSR suppression, an extra controller should be implemented in the conventional controller of the SSSC. The main structure of the proposed auxiliary damping controller, the conventional lead-lag controller, is shown in Figure 7. As seen in the figure,  $\Delta\omega [p.u]$  has been implemented as an additional signal to mitigate the unstable modes. The auxiliary SSRD controller consists of 5 blocks: a washout filter, 2 phase compensator blocks, a limiter block, and a gain block. The washout filter is used to prevent the controller from responding to the steady-state changes of the input signal. The phase compensator block presents the suitable lead-lag features to produce the damping torque. The limiter block tends to restrict the output of the controller when it is going to decrease or increase from a specific range. The output of the SSRD controller is therefore sent to the conventional controller of SSSC in Figure 5 in order to modulate the reference settings of the SSSC.

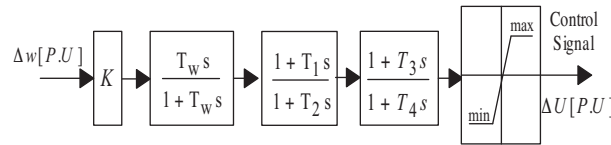


Figure 7. SSRD controller block diagram.

In order to ameliorate the overall system dynamic stability in a robust way, the parameters of the proposed CDC should be tuned. The parameter  $T_w$  and limiter parameter are set manually, but the other parameters will be optimized by the PSO algorithm in order to yield the SSR suppression. In this study, an objective function that comes from the speed deviation of the rotor shaft is utilized in order to yield the fittest output parameters for the SSRD controller. The mentioned objective function is an integral of time multiplied by the absolute value of the speed deviation and can be expressed by:

$$J = \int_0^{t_{sim}} t \cdot |\Delta\omega|.dt, \tag{5}$$

where  $t_{sim}$  is the simulation time and  $\Delta\omega$  is the speed deviation of the rotor shaft in the IEEE SBM. The main aim of the optimization is to minimize the objective function due to some constraints shown below.

$$K^{min} \leq K \leq K^{max}$$

$$\begin{aligned}
 T_1^{min} &\leq T_1 \leq T_1^{max} \\
 T_2^{min} &\leq T_2 \leq T_2^{max} \\
 T_3^{min} &\leq T_3 \leq T_3^{max} \\
 T_4^{min} &\leq T_4 \leq T_4^{max}
 \end{aligned}
 \tag{6}$$

The PSO algorithm searches for the optimal values of the parameters above in the range of [0.001–200] for  $K$  and [0.001–3] for  $T_1, T_2, T_3, T_4$ . With implementation of the time-domain simulation model of the power system in the simulation period, the objective function is computed, and after reaching the specified criterion, the optimal parameters of the controller will be achieved. Parameters of the proposed PSO-based SSRD are as follows:  $K = 5, T_W = 2, T_1 = 0.9106, T_2 = 0.0497, T_3 = 0.3532, T_4 = 0.7757, \max = 0.15,$  and  $\min = -0.15$ .

### 3.2. FLDC design for SSR mitigation

Generally, the power system has nonlinear behavior, so the FLCs, which are nonlinear in nature, are implemented to yield a robust performance under disturbances. Unlike the crisp logic in Boolean theory that implements just 2 orders of logic (0,1), fuzzy logic can extensively select infinite logic levels from 0 to 1 to resolve problems in adverse situations like disturbances or failures. It has been available as a control methodology for over 3 decades and its application to engineering control systems is well proven. In a sense, fuzzy logic is a logical system that is an extension of multivalued logic, although in character it is quite different. It has become popular due to the fact that human reasoning and thought formation are linked very strongly with the ways in which fuzzy logic is implemented. In the power system area, it has been used in stability studies, load frequency control, unit commitment, and reactive compensation in the distribution network [19].

Here the proposed controller is designed based on Mamdani’s inference engine. Fuzzification, defuzzification, rule base, and inference engine are essential parts of this controller, which are classified as follows:

- **Fuzzification:**

This part of the FLC involves mapping the fuzzy variables to crisp numbers used by the fuzzy controller. Fuzzification executes a membership grade to translate the numeric values of error into linguistic value. In this paper, fuzzy input includes 2 input signals, namely speed deviation  $\Delta\omega [p.u]$  and its derivative  $\frac{d\Delta\omega}{dt}$ . By studying the behavior of these 2 input signals in different situations before and after the fault, fuzzy sets for the fuzzy controller are designed. The main configuration of the FLDC is illustrated in Figure 8.

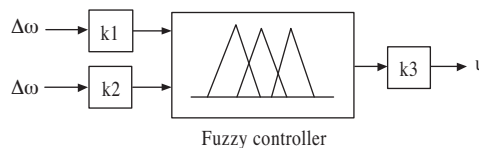


**Figure 8.** The main configuration of FLDC.

The membership functions for inputs and output of the FLDC are depicted in Figure 9. For each input and output, 7 membership functions are introduced and tuned based on simulation and knowledge of the power system.



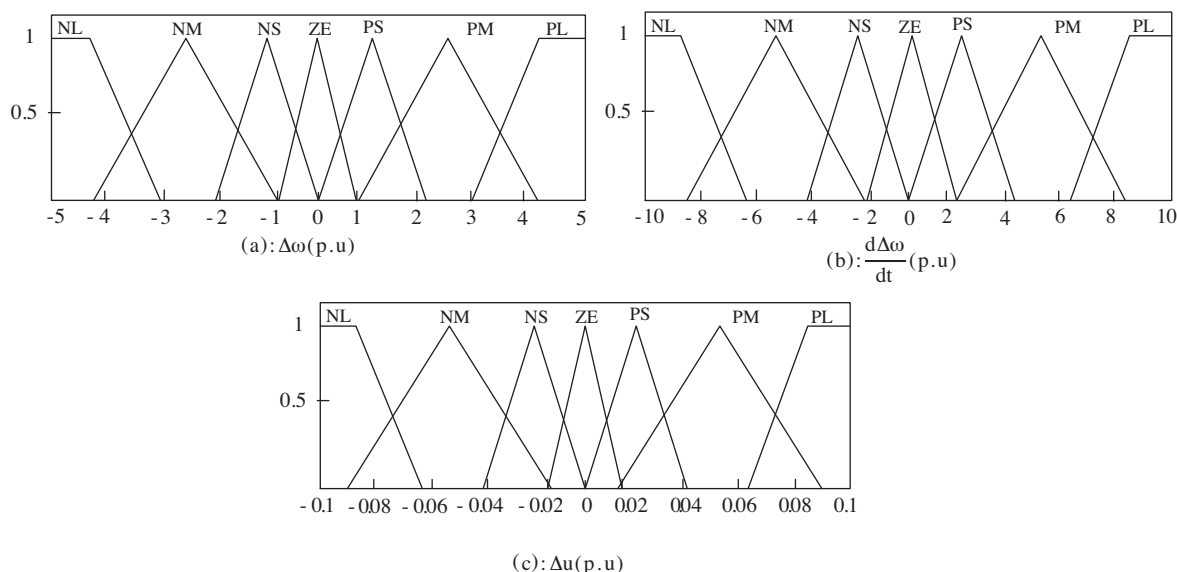


**Figure 9.** Triangular membership functions for inputs and output fuzzy sets of the FLDC.

• **Rule base and inference engine:**

The rule base is the heart of fuzzy controller. The fuzzy control strategy is realized in the inference engine that is a rule base including all possible combinations of inputs and proper outputs for each of them. The rule base with 2 proposed inputs is shown in the Table.

**Table.** Rule base of the FLDC.

$\Delta\omega$ $\frac{d\Delta\omega}{dt}$	<i>PL</i>	<i>PM</i>	<i>PS</i>	<i>ZE</i>	<i>NS</i>	<i>NM</i>	<i>NL</i>
<i>PL</i>	<i>PL</i>	<i>PL</i>	<i>PL</i>	<i>PL</i>	<i>PM</i>	<i>PS</i>	<i>ZE</i>
<i>PM</i>	<i>PL</i>	<i>PL</i>	<i>PM</i>	<i>PM</i>	<i>PS</i>	<i>ZE</i>	<i>NS</i>
<i>PS</i>	<i>PL</i>	<i>PM</i>	<i>PS</i>	<i>PS</i>	<i>ZE</i>	<i>NS</i>	<i>NM</i>
<i>ZE</i>	<i>PL</i>	<i>PM</i>	<i>PS</i>	<i>ZE</i>	<i>NS</i>	<i>NM</i>	<i>NL</i>
<i>NS</i>	<i>PM</i>	<i>PS</i>	<i>ZE</i>	<i>NS</i>	<i>NS</i>	<i>NM</i>	<i>NL</i>
<i>NM</i>	<i>PS</i>	<i>ZE</i>	<i>NS</i>	<i>NM</i>	<i>NM</i>	<i>NL</i>	<i>NL</i>
<i>NL</i>	<i>ZE</i>	<i>NS</i>	<i>NM</i>	<i>NM</i>	<i>NL</i>	<i>NL</i>	<i>NL</i>

In the Table, the abbreviations are as follows: NL, negative large; NM, negative medium; NS, negative small; ZE, zero; PS, positive small; PM, positive medium; and PL, positive large. These rules are chosen based on human reasoning. The inference engine implemented here follows Mamdani’s inference engine. Two examples of the rule base are included as follows for better understanding:

Rule 1: If  $\Delta\omega$  is PL and  $\frac{d\Delta\omega}{dt}$  is NM, then FLC output should be PS

Rule 2: If  $\Delta\omega$  is NS and  $\frac{d\Delta\omega}{dt}$  is ZE, then FLC output should be NS.

Rules and membership functions are defined and tuned so that the appropriate signal provides for alleviating the oscillations.

• Defuzzification

In this part, a ‘crisp’ numeric value, which is used as a control input for power system, is generated by outputs of fuzzy rules. Once the input variables are fuzzified and sent to the fuzzy rule base, the output of rule base is then aggregated and defuzzified. Aggregation means that all of the output fuzzy sets are added in logical way. A crisp control signal is then produced. A common method, namely the centroid method, is implemented for this purpose, where the control signal is calculated as:

$$\Delta u(k) = \frac{\sum_{i=1}^n F_i S_i}{\sum_{i=1}^n F_i} \tag{7}$$

where  $F_i$  is the membership grade and  $S_i$  is the membership function’s singleton position.

4. Simulation results

To validate the performance of the proposed controllers, time-domain simulations are performed using a nonlinear system model and the responses of the network to different disturbances. The following case studies are undertaken for evaluating the performance of the proposed controller in the mitigation of SSR.

Case 2: A 3-phase fault of 0.0168 s in duration is simulated at point A (see Figure 1). The performance of the PSO-based CDC and FLDC in damping the SSR is presented in Figures 10a and 10b, respectively. In this case, the performances of each control scheme are almost the same. This is because the parameters of all of the controllers are tuned at this operating condition with the previously mentioned fault.

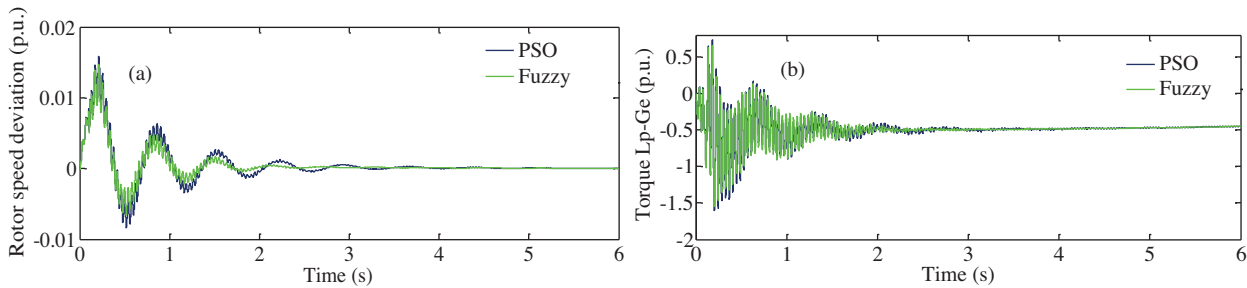


**Figure 10.** Simulation results for the comparison between PSO-based CDC and FLDC in case 2: a) generator rotor speed deviation in p.u., b) the torque between the low-pressure turbine and generator in p.u.

Case 3: The duration of the same fault is increased from 0.0168 s to 0.0268 s at the previous operating conditions. Figure 11a and 11b illustrate the generator rotor speed deviation and torsional torque between the generator and low-pressure turbine with consideration of the FLDC and PSO-based CDC. These figures expose the ability of both designed controllers in alleviating the SSR. From these figures, it can be noted that the operation of the SSSC enhanced with the FLDC prepares a better damping in comparison with the SSSC enhanced with the PSO-based CDC.

Case 4: The fault duration is further increased to 272.5 ms at the same operating conditions. The simulation results are presented in Figure 12. Under these condition, it is found that the PSO-based CDC scheme is unstable, whereas the FLDC scheme is stable in its operation. Therefore, the proposed FLDC for SSSC provides a higher critical clearing time compared to the PSO-based CDC. This increase in critical clearing

time will enable more time for the opening of the circuit breaker following a fault. It also increases the transient fault duration that the system can withstand.

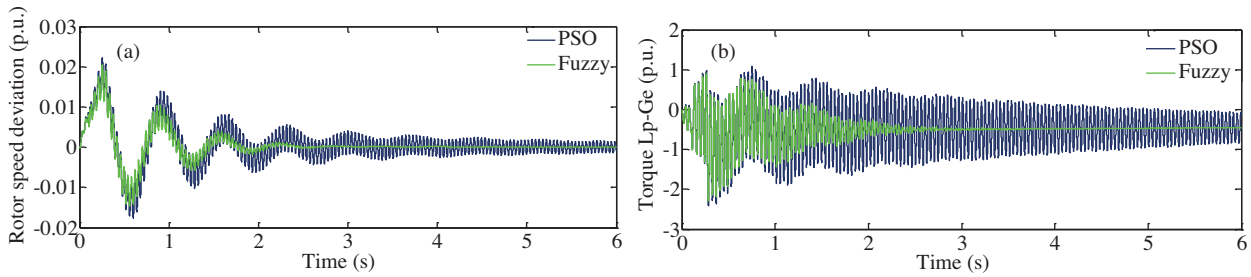


**Figure 11.** Simulation results for the comparison between PSO-based CDC and FLDC in case 3: a) generator rotor speed deviation in p.u., b) the torque between the low-pressure turbine and generator in p.u.

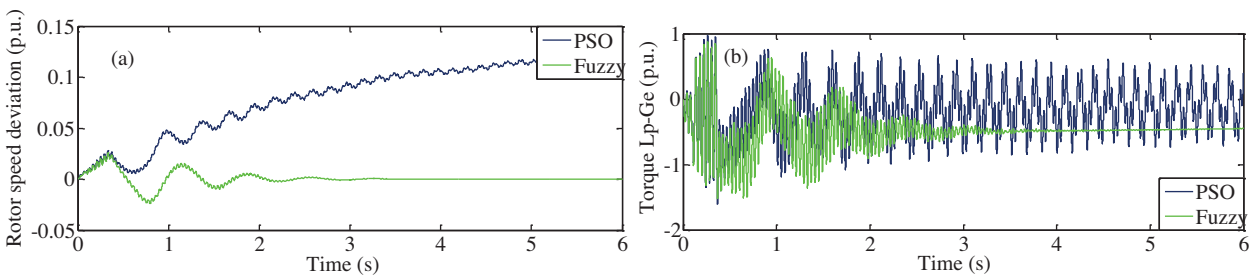


**Figure 12.** Simulation results for the comparison between PSO-based CDC and FLDC in case 4: a) generator rotor speed deviation in p.u., b) the torque between the low-pressure turbine and generator in p.u.

Case 5: The operating condition of the studied power system in p.u. is changed to a higher power level of  $P = 0.9$  p.u. and  $Q = 0.3$  p.u., but the duration of the fault is the same as in case 1 (a 3-phase fault of 0.0168 s in duration). Simulation results for this operation condition are presented in Figure 13. It can be noted that, at these operating conditions, both the CDC and the FLDC can stabilize the system after the fault, but, because of changing the system operation point, the performance of the CDC declines. This is because the parameters of the PSO-based CDC are tuned in case 1's operating conditions and the parameters are not valid when the system's operation condition changes, but the designed FLDC can greatly change its operation condition even if the system's operating point alters greatly. It should be noted that, in this situation, the PSO-based damping controller should be reoptimized in order to yield convincing results. Furthermore, the FLDC performance is not related to the system conditions and it will act properly even when the power system's configuration and operation point is changed or in the event of severe disturbances (case 4).

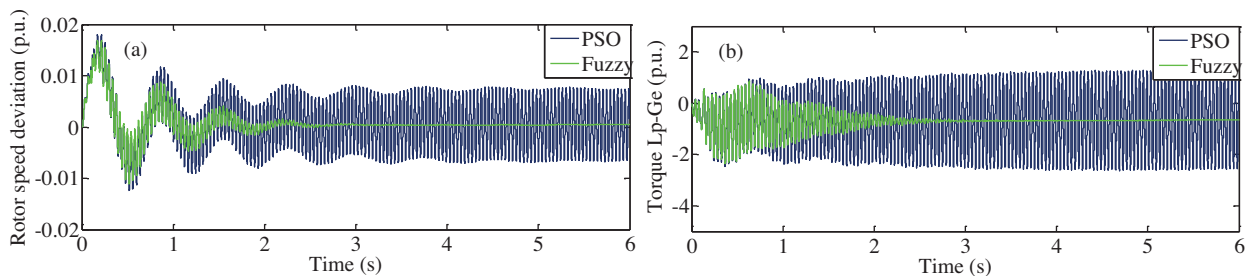


**Figure 13.** Simulation results for comparison between PSO-based CDC and FLDC in case 5: a) generator rotor speed deviation in p.u., b) the torque between the low-pressure turbine and generator in p.u.

## 5. Conclusion

A FLC approach for SSR mitigation using a SSSC has been addressed in this work. A CDC has been also designed to assess the FLDC capabilities and to compare the results of mitigation with the FLDC. To obtain a comprehensive understanding of this case, FFT analysis has been employed. It has been found that for the selected level of series compensation, the second mode (with the corresponding frequency around 25 Hz) has been the most dominant in making the system unstable. The parameters of the CDC have been optimized with the aid of the PSO algorithm, yielding superior damping of the CDC and also to compare with the FLDC comprehensively. The results of dynamical performances have shown that in a nominal condition, both damping controllers (CDC and FLDC) exhibit acceptable performances for SSR mitigation. The performance of the CDC is reduced for any changes of the system's operating point or fault duration. From another aspect, the CDC is not capable of damping the oscillations and subsequently stabilizes the system for large disturbances. The reason can be explored within the optimization of the PSO parameters for one condition, based on the CDC, where the parameters optimized would not be valid for any changes of the system operation condition. In contrast, the FLDC provides significant stable performances and is able to dampen SSR over a wide range of operation conditions. The results obtained indicate a highly effective controller developed for the fault duration and the improvement of the fault clearing time.

## References

- [1] T.J.E. Miller, *Reactive Power Control in Electric Systems*, New York, John Wiley & Sons, 1982.
- [2] IEEE Subsynchronous Resonance Working Group, "First benchmark model for computer simulation of subsynchronous resonance", *Power Apparatus and Systems*, Vol. 96, pp. 1565–1572, 1977.
- [3] IEEE Subsynchronous Resonance Working Group, "Terms, definitions and symbols for subsynchronous oscillations", *IEEE Transactions on Power Apparatus and Systems*, Vol. 104, pp. 1326–1334, 1985.
- [4] D.N. Walker, C.E.J. Bowler, R.L. Jackson, D.A. Hodges, "Results of subsynchronous resonance test at Mohave", *IEEE Transactions on Power Apparatus and Systems*, Vol. 5, pp. 1878–1889, 1975.
- [5] A.M. El-Serafi, M.Y. Niamat, E. Haq, "Contribution of power system stabilizers to the damping of torsional oscillations of large turbo generators", *Journal of Electric Power Components and Systems*, Vol. 11, pp. 451–464, 1986.
- [6] M. Bongiorno, J. Svensson, L. Angquist, "On control of static synchronous series compensator for SSR mitigation", *IEEE Transactions on Power Electronics*, Vol. 23, pp. 735–743, 2008.
- [7] R.K. Varma, S. Auddy, Y. Semsedini, "Mitigation of subsynchronous resonance in a series-compensated wind farm using FACTS controllers", *IEEE Transactions on Power Delivery*, Vol. 23, pp. 1645–1654, 2008.
- [8] F.D. de Jesus, E.H. Watanabe, L.F.W. de Souza, J.R. Alves, "SSR and power oscillation damping using gate-controlled series capacitors (GCSC)", *IEEE Transactions on Power Delivery*, Vol. 22, pp. 1806–1812, 2007.
- [9] M.S. El-Moursi, B. Bak-Jensen, M.H. Abdel-Rahman, "Novel STATCOM controller for mitigating SSR and damping power system oscillations in a series compensated wind park", *IEEE Transactions on Power Electronics*, Vol. 25, pp. 429–441, 2010.
- [10] M. Khalilian, M. Mokhtari, S. Golshannavaz, D. Nazarpour, "Distributed static series compensator (DSSC) for subsynchronous resonance alleviation and power oscillation damping", *European Transactions on Electrical Power*, Vol. 22, pp. 589–600, 2012.
- [11] K. Kabiri, S. Henschel, J.R. Martí, H.W. Dommel, "A discrete state-space model for SSR stabilizing controller design for TCSC compensated systems", *IEEE Transactions on Power Delivery*, Vol. 20, pp. 466–474, 2005.
- [12] D. Rai, S.O. Faried, G. Ramakrishna, A. Edris, "Hybrid series compensation scheme capable of damping subsynchronous resonance", *IET Generation, Transmission and Distribution*, Vol. 4, pp. 456–466, 2010.

- [13] L. Gyugyi, C.D. Schauder, K.K. Sen, "Static synchronous series compensator: a solid-state approach to the series compensation of transmission lines", *IEEE Transactions on Power Delivery*, Vol. 12, pp. 406–417, 1997.
- [14] K.K. Sen, "SSSC: Static synchronous series compensator: theory, modeling and application", *IEEE Transactions on Power Delivery*, Vol. 13, pp. 241–246, 1998.
- [15] G.N. Pillai, A. Ghosh, A. Joshi, "Torsional oscillation studies in an SSSC compensated power system", *Electric Power Systems Research*, Vol. 55, pp. 57–64, 2000.
- [16] G.N. Pillai, A. Ghosh, A. Joshi, "Robust control of SSSC to improve torsional damping", in *Proceedings of 38th IEEE Power Engineering Society Winter Meeting*, Vol. 3, pp. 1115–1120, 2011.
- [17] M. Bongiorno, L. Angquist, J. Svensson, "A novel control strategy for subsynchronous resonance mitigation using SSSC", *IEEE Transactions on Power Delivery*, Vol. 23, pp. 1033–10041, 2008.
- [18] M. Bongiorno, J. Svensson, L. Angquist, "On control of static synchronous series compensator for SSR mitigation", *IEEE Transactions on Power Electronics*, Vol. 23, pp. 735–743, 2008.
- [19] H.J. Zimmermann, *Fuzzy Set Theory and its Applications*, 3rd ed., Dordrecht, Kluwer Academic Publishers, 1996.
- [20] M. Zarghami, M.L. Crow, S. Jagannathan, "Nonlinear control of FACTS controllers for damping interarea oscillations in power systems", *IEEE Transactions on Power Delivery*, Vol. 25, pp. 3113–3121, 2010.
- [21] T. Hiyama, "Rule-based stabilizers for multi-machine power system", *IEEE Transactions on Power Systems*, Vol. 5, pp. 403–411, 1990.
- [22] P.K. Dash, S. Morris, S. Mishra, "Design of a nonlinear variable-gain fuzzy controller for FACTS devices", *IEEE Transactions on Control Systems Technology*, Vol. 12, pp. 428–438, 2004.
- [23] M.R.A. Pahlavani, H.A. Mohammadpour, "Damping of sub-synchronous resonance and low-frequency power oscillation in a series-compensated transmission line using gate-controlled series capacitor", *Electric Power Systems Research*, Vol. 81, pp. 308–317, 2011.
- [24] A.L. Do Bomfim, G.N. Taranto, D.M. Falcão, "Simultaneous tuning of power system damping controllers using genetic algorithms", *IEEE Transactions on Power Systems*, Vol. 15, pp. 163–169, 2000.
- [25] J. Kennedy, R. Eberhart, Y. Shi, *Swarm Intelligence*, San Francisco, Morgan Kaufman Publishers, 2001.
- [26] S.L. Ho, S. Yang, G. Ni, E.W. Lo, H.C.C. Wong, "A particle swarm optimization-based method for multiobjective design optimizations", *IEEE Transactions on Magnetics*, Vol. 41, pp. 1756–1759, 2005.
- [27] H. Shayeghi, H.A. Shayanfar, S. Jalilzadeh, A. Safari, "Design of output feedback UPFC controllers for damping of electromechanical oscillations using PSO", *Energy Conversion Management*, Vol. 50, pp. 2554–2561, 2009.
- [28] IEEE Subsynchronous Resonance Working Group, "Second benchmark model for computer simulation of subsynchronous resonance", *IEEE Transactions on Power Apparatus and Systems*, Vol. 104, pp. 1057–1066, 1985.
- [29] N.G. Hingorani, L. Gyugyi, *Understanding FACTS: Concepts and Technology of Flexible AC Transmission Systems*, New York, Wiley-IEEE Press, 2000.